Carrier capture in ultrathin InAs/GaAs quantum wells

J. Brübach,* A. Yu. Silov, J. E. M. Haverkort, W. van der Vleuten, and J. H. Wolter
COBRA Interuniversity Research Institute, Eindhoven University of Technology, Department of Physics, P.O. Box 513, 5600 MB Eindhoven, The Netherlands
(Received 21 December 1999)

The carrier capture into ultrathin InAs layers embedded in a GaAs matrix has been investigated by time-resolved two-wavelength pump-probe phototransmission at 4.2 K. Using an InAs thickness of 1.2 monolayers, we observe switching of the carrier relaxation from optical to acoustic phonon emission. At the light-hole (lh) exciton transition we find a constant capture time of 20 ps. In contrast, the capture time decreases abruptly from 50 ps to 22 ps within the heavy-hole (hh) exciton transition as the energy separation between lh and hh states exceeds the threshold for GaAs LO phonon emission. The combination of both characteristics provides strong evidence for a two-step capture process of the holes. First the holes are captured by the weakly confined lh state and then they cool down to the hh state. We calculated the transient bleaching of the excitonic absorption considering both phase-space filling and exciton screening. The calculations show in agreement with the measurements that the phototransmission transients directly reflect the population of the confined InAs states only at excitation densities below 3×10^{8} cm^{-2}. At larger excitation densities, the phototransmission rise time becomes significantly smaller than the capture times whereas its decay time appears longer than the carrier lifetime.

I. INTRODUCTION

During recent years, great efforts have been directed towards the investigation of the optical properties of monolayer (ML) thick InAs layers embedded into a GaAs bulk matrix.[1–4] One of the most striking optical properties of these ultrathin InAs/GaAs quantum wells is the appearance of a strong photoluminescence (PL) line below the GaAs band gap. This PL is well known to arise from the recombination of hh excitons bound to the InAs layer.[5,6] The peak intensity of the InAs PL was found to be higher than the excitonic PL of the surrounding GaAs matrix[7–9] by a factor 100–500 suggesting a very efficient carrier capture by the InAs layer.

For capture times in relatively thin heterostructures only a few comparable values are available. Calculations from Brum and Bastard,[10] based on their state-of-the-art quantum-mechanical capture model for electrons and holes, show a capture time of 45 ps for a shallow 50-Å-wide GaAs quantum well with 500-mm $Al_{0.18}Ga_{0.82}As$ barriers. A recent adaptation of their theory by Heller and Bastard[11] for exciton capture reveals capture times of less than 1.2 ps for a shallow, but 200-Å-wide GaAs/AlGaAs quantum well. Blom *et al.*[12] found an ambipolar capture time of 22 ps for a 26-Å-GaAs quantum well centered in a 1000-Å-wide $Al_{0.3}Ga_{0.7}As$ separate confinement heterostructure, and recently capture times below 1 ps were reported in a 25-Å-wide Be δ-doped structure.[13] For ultrathin InAs/GaAs quantum wells, the only published value for the carrier capture time is an estimate of 20 ps from Brandt *et al.*[14] based on the ratio of the PL intensities of the InAs layer hh exciton transition and the GaAs band-edge emission. Experimental data for the capture times in ultrathin InAs layers, however, are still lacking.

In this work we present an experimental study of the carrier capture in a single ultrathin InAs layer embedded in a GaAs matrix. The capture times were measured by time-resolved two-wavelength pump-probe phototransmission. The choice of an InAs layer thickness of 1.2 ML targeted the interesting situation where the hh and lh states are both confined, and their difference in confinement energy amounts to approximately one GaAs LO phonon. By measuring the spectral dependence of the capture times in the vicinity of the hh and lh exciton transitions, we focused in particular on the role of the confined lh state in the capture process. We found a constant capture time of 20 ps at the lh exciton transition. In contrast, within the hh exciton transition the capture time increased abruptly from 22 ps to 50 ps as soon as the hh-lh separation became smaller than the GaAs LO phonon energy. This suggests that the carrier capture in ultrathin InAs layers occurs in a two-step process with the confined lh level acting as an intermediate state.

When using phototransmission (PT) for the capture measurements, one needs to clarify to what extent the observed bleaching of the excitonic absorption reflects the true evolution of the confined states population. For that reason, we calculated the transient PT taking into account the contributions of both phase-space filling and exciton screening. Realistic values for the in-plane hh and lh effective masses were obtained from the calculation of the in-plane dispersion in the 1.2-ML-thick InAs layer. The required exciton dimensionalities and effective Bohr radii were derived from the measured hh and lh exciton binding energies. Our calculations and experiments show in agreement that the transient PT directly reflects the population in the confined states only for excitation densities lower than 3×10^{8} cm^{-2}. In our capture experiments the excitation density was kept at 2×10^{8} cm^{-2}.

The paper is organized as follows. In Sec. II we discuss the sample growth, its characterization by PL and x-ray diffraction, and the time-resolved two-wavelength pump-probe phototransmission setup. The transient PT in ultrathin InAs layers is calculated in Sec. III. There we also demonstrate the

impact of nonlinearities in the bleaching as a function of excitation density on the correlation between the evolution of the population in the confined states and the transient PT as observed in the experiments. The results for the carrier capture in ultrathin InAs layers are presented in Sec. IV. For the discussion of the capture times at the hh and lh exciton transitions we use rate equations as described in Appendix A. In Appendix B we present a systematic parameter study of the capture and relaxation times substituted into the rate equations.

II. EXPERIMENT

The sample under investigation was synthesized by conventional molecular beam epitaxy on CrO-doped semi-insulating (001) GaAs substrate. After oxide desorption, the layer sequence started with a 0.4-μm GaAs buffer layer, followed by a 350-Å GaAs layer, within which the substrate temperature was lowered from 630 °C to 450 °C. At this lower temperature the InAs layer, and subsequently 5 ML of GaAs were deposited. Before and after the InAs layer a 1-s growth interruption was introduced. While growing the next 565 Å of GaAs, the substrate temperature was returned to 630 °C. Finally, the structure was capped with a 300-Å $Al_{0.33}Ga_{0.67}As$ window and a 170-Å GaAs layer.

The thickness of the InAs layer was determined by high-resolution x-ray diffraction in (004) geometry.[15] From simulations of the rocking curves based on the dynamical theory we found an InAs layer thickness of 1.2 ± 0.1 ML, assuming 6.8% compressive strain. The x-ray study also revealed that more than 80% of the deposited InAs is confined within a single atomic plane.

The sample was characterized with standard PL measurements at 4.2 K. Below the GaAs band gap at 1.445 eV the strong PL line of the InAs hh exciton transition was observed. The peak intensity ratio between the InAs hh exciton emission and the GaAs exciton at 1.515 eV was approximately 650, demonstrating the efficient trapping of carriers by the InAs layer.

The capture times were measured with picosecond time-resolved two-wavelength pump-probe phototransmission, which allows a direct spectral control of both the initial and final states involved in the capture process. Moreover, by tuning the probe wavelength through the hh and lh exciton transitions, the relaxation of the captured holes within the InAs layer can be traced independently. The laser system consisted of two double jet dye lasers, which were synchronously pumped by a frequency doubled Nd:YAG laser. The excitation wavelength of the pump laser was fixed to 682 nm (1.818 eV) and its pulse width (FWHM) was better than 1 ps. For the generation of the probe pulses, a mixture of Styryl 8 and Styryl 9 was used to provide a spectral tuneability from 780 nm to 900 nm. Over the whole spectral range the pulse width was below 1.5 ps. To achieve a compromise between optimum spectral and temporal resolution in the capture experiments, both dye lasers were operated with single-plate birefringent filters, which provided a spectral resolution of 0.8 meV. After the beams passed a variable delay line, they were focused onto the sample in near backscattering geometry with the spot size of the probe beam being four times smaller than the pump beam. Consequently, the excitation density can be assumed as homogenous and systematic errors due to lateral carrier diffusion can be excluded. The sample was mounted in a He flow cryostat and held by paper frames to avoid any possible source of external strain. By modulating the pump beam, the induced transmission change was measured as a function of pump and probe delay utilizing a conventional Si pin-diode and standard lock-in technique. During the experiments the cross correlation of pump and probe beams, which marks the position of zero delay and whose temporal width equals to the time resolution of the setup, was monitored. Due to remaining jitter of the pump and probe beams the FWHM of the cross correlation was limited to 2 ps. Finally, the intensity ratio between pump and probe beam was kept below 50.

III. ESTIMATES FOR THE LINEAR RANGE OF THE PHOTOTRANSMISSION

The most common criticism with respect to the interpretation of carrier capture experiments is the query over the extent to which the measured transients directly reflect the evolution of the population in the states associated with the optical transition. When using time-resolved PT, the evolution of the population in the confined states of the InAs layer is transformed into the PT transients through the reduction in exciton oscillator strength as a function of excitation density. Depending on the dominating bleaching mechanism, the decrease in excitonic absorption might have a strong nonlinear dependence on the carrier concentration, altering the observed rise and decay times with respect to the capture and recombination times of the true population. In addition, the amount of bleaching differs for hh and lh excitons due to their different in-plane effective masses. It is thus important to find a model that correlates the temporal evolution of the population in the confined states with the transient PT of the associated excitonic states or, alternatively, experimental conditions where the measured PT transients directly reflect the population.

Experimentally, rise and decay times of the population are conserved in the PT transient for excitation densities, which provide a linear change in the magnitude of the PT. Figure 1(a) displays the PT transients at the peak position of the hh exciton transition at 1.451 eV, measured at different excitation densities, and Fig. 1(b) shows the magnitude of the PT observed in the maximum of the transient as a function of excitation density. The solid line in Fig. 1(b) represents the calculations of the transient PT discussed below. As can be seen from Fig. 1(b), for excitation densities of up to $3 \times 10^8\,\mathrm{cm}^{-2}$ the magnitude of the PT increases almost proportionally with the excitation density, and consequently the PT transients in Fig. 1(a) exhibit virtually the same rise and decay times. In contrast, at excitation densities larger than $10^9\,\mathrm{cm}^{-2}$ the magnitude of the PT significantly starts to saturate. At these excitation densities the PT transients show a slightly diminished rise time whereas the decay time appears to increase. For the largest excitation density of $7 \times 10^{10}\,\mathrm{cm}^{-2}$ the maximum of the transient evolves into a broad plateau. It can be concluded from these measurements that the PT transients in the investigated InAs layer directly reflect the population in the confined states only for excitation densities up to $3 \times 10^8\,\mathrm{cm}^{-2}$.

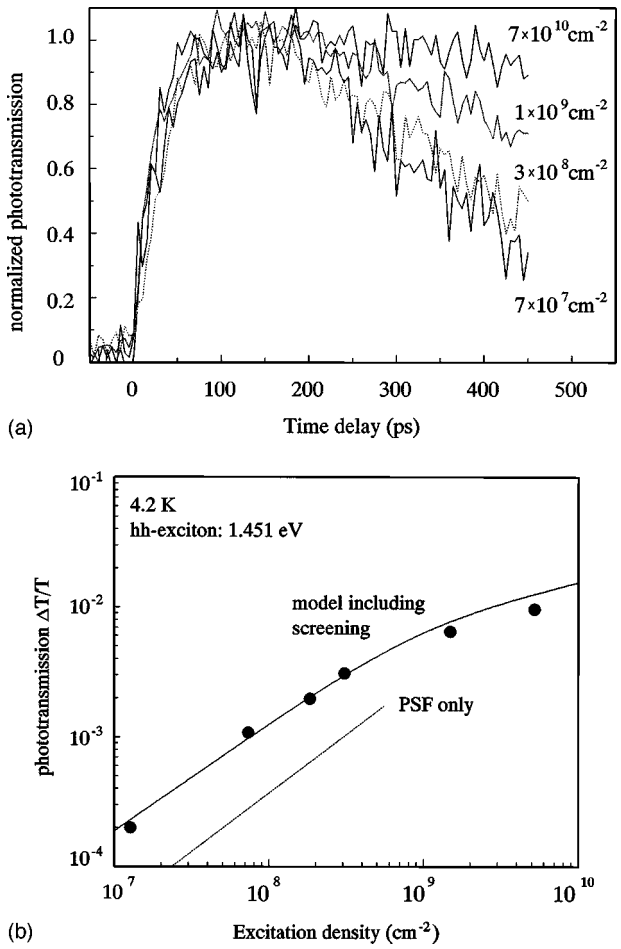

FIG. 1. (a). Normalized phototransmission transients measured at the peak position of the hh exciton transition at 1.451 eV for different excitation densities. (b). Measured (symbols) and calculated (solid line) magnitude of the phototransmission at the maximum of the transient as a function of excitation density. The individual contribution of phase-space filling (PSF) is indicated by the dotted line.

For a theoretical treatment of the observed PT behavior, we assume that the insertion of an InAs monolayer into a GaAs matrix introduces single electron, hh, and lh states in the GaAs band gap. The confined states give rise to the formation of hh and lh excitons bound to the InAs, and their population by photogenerated carriers leads to a bleaching of the excitonic absorption. The in-plane dispersion of the confined hh and lh states of the InAs layer can be calculated within the framework of the δ-potential model by a two-band Luttinger Hamiltonian in a spherical approximation described elsewhere.[16] We find that for $k_{\parallel}$ values of up to the same order as the inverse exciton Bohr radii the in-plane dispersion of the hh and lh states can be described in parabolic approximation with an effective mass of $m^*_{\parallel,\mathrm{hh}}=0.155\times m_0$ for the hh states and $m^*_{\parallel,\mathrm{lh}}=0.362\times m_0$ for the lh states. The hh and lh effective masses in growth direction are found to be $m^*_{\mathrm{hh}}=m_0/(\gamma_1-2\gamma_2)=0.3774\times m_0$ and $m^*_{\mathrm{lh}}=m_0/(\gamma_1+2\gamma_2)=0.0905\times m_0$, with the Luttinger parameters γ_1 and γ_2 fixed to the values of the GaAs barrier.

The hh and lh exciton binding energies in the absence of photogenerated carriers are calculated within the framework of the zero-radius potential model.[17,3] For a 1.2-ML-thick InAs layer one finds an exciton binding energy of 11 meV for the hh exciton and 6 meV for the lh exciton. This is in agreement with our experimental results, obtained from PLE and temperature-dependent PL measurements,[16] of 10 meV for the hh exciton binding energy and 5.5 meV for the lh exciton binding energy. For the dimensionality parameter D of the excitons, defined by $E_x=4D\times R^*$, where R^* denotes the Rydberg energy and E_x the measured exciton binding energy, we find $D=0.66$ for the hh excitons and $D=0.30$ for the lh excitons. This demonstrates that the hh excitons have a $2D$ character, whereas the lh excitons are $3D$. Finally, the Bohr radius a^* of the hh and lh exciton amounts to 90 Å and 115 Å, respectively.

The bleaching of the excitonic absorption due to phase-space filling[18] increases strictly linear as a function of excitation density N, for $N\leqslant N_s$. The saturation parameter $1/N_s$ represents an area occupied by a photogenerated electron-hole pair, which cannot sustain more excitons. For the relevant case of a nondegenerate electron-hole population, which is distributed within the LO phonon energy $\hbar\omega_{\mathrm{LO}}$ above the GaAs band edges, the saturation parameter amounts to $1/N_s=8\pi a^{*2}E_x/\hbar\omega_{\mathrm{LO}}$. For the hh excitons N_s can be estimated with $1.7\times10^{11}\,\mathrm{cm}^{-2}$. If phase-space filling would be the only bleaching mechanism, the measured PT transients should directly reflect the population in the confined InAs states for excitation densities up to this value for N_s. Our excitation density-dependent measurements of the PT, however, shown in Figs. 1(a) and 1(b), already exhibit a deviation from linear behavior for excitation densities larger than $3\times10^8\,\mathrm{cm}^{-2}$. This behavior can only be explained when screening of the Coulomb interaction is taken into account.

To correct for the effect of screening on the bleaching we use the potential[19]

$$V_s(r)=-\frac{e^2}{4\varepsilon\varepsilon_0 r}\left\{1-\frac{1}{2\pi\kappa_s}[H_0(\kappa_s r)-J_0(\kappa_s r)]\right\}, \quad (1)$$

where κ_s denotes the inverse screening length, and H_0 and J_0 are the Struve function and Bessel function of the second kind, respectively. For distances $r\ll\kappa_s^{-1}$ this potential behaves like a Coulomb potential, whereas for $r\gg\kappa_s^{-1}$ it falls off as r^{-3}. Following Ref. 20, the change in exciton binding energy and oscillator strength of the hh and lh excitons was calculated in a variational approach. Using a trial wave function for the exciton ground state $\psi_x(r)=\lambda/\sqrt{2\pi}\times\exp(-\lambda r/2)$, the energy expectation value was minimized with respect to the variational parameter λ. The exciton binding energies were subsequently corrected by the dimensionality parameter in order to match the results for the limiting case $N\to0$ with E_x as found by the zero-radius potential model in the absence of photogenerated carriers. The inverse screening length entering Eq. (1) was obtained from the Debye model for $2D$ semiconductors[20,21] as

$$\kappa_s=\frac{2}{a^*}\left\{\frac{m^*_{\parallel,e}}{\mu^*_{\parallel}}[1-\exp(-n_e\pi\hbar^2/m^*_{\parallel,e}k_BT)] + \frac{m^*_{\parallel,h}}{\mu^*_{\parallel}}[1-\exp(-p_h\pi\hbar^2/m^*_{\parallel,h}k_BT)]\right\}, \quad (2)$$

where n_e and p_h denote the carrier concentrations and $\mu_\parallel^*$ is the reduced in-plane effective mass. As can be seen from Eq. (2), the inverse screening length for both hh and lh excitons increases linearly up to excitation densities of approximately $5\times10^8\,\mathrm{cm}^{-2}$. In this range the inverse screening length becomes independent on the effective masses, i.e., the contributions to screening from captured electrons and holes are equal. For larger excitation densities the inverse screening length starts to deviate from linear behavior, and at $5\times10^{10}\,\mathrm{cm}^{-2}$ it reaches the saturation limit of $\kappa_s = 2/a^*[(m_{\parallel,e}^*+m_{\parallel,h}^*)/\mu_\parallel^*]$. In the nonlinear regime of κ_s the individual contributions of captured electrons and holes to the screening diverge with the result that the PT becomes more sensitive to the electron capture than to the capture of a hole. In the regime where screening becomes density independent, the exciton binding energy saturates at a value of $0.56\times R^*$, as predicted by random-phase approximation,[22] reflecting the persistence of the two-dimensional (2D) exciton ground state even at high carrier concentrations.[23]

The calculations of the PT incorporating both phase-space filling and exciton screening are displayed in Figs. 1(b) and 2, respectively. To facilitate direct comparison with the experiments, the calculations were performed at the peak position of the hh exciton transition. The solid lines in Fig. 1(b) represent the calculated PT in the maximum of the transient as a function of excitation density. Calculations and measurements show in agreement that up to $3\times10^8\,\mathrm{cm}^{-2}$ the bleaching increases almost linearly with excitation density, but starts to saturate at higher densities. This nonlinear behavior is caused by saturation of the inverse screening length suggesting that the bleaching results predominantly from exciton screening. It can be seen from Fig. 1(b) that at excitation densities below $10^9\,\mathrm{cm}^{-2}$ the contribution from phase-space filling is 2–4 times smaller than the contribution from exciton screening. This is in agreement with the work of Snelling *et al.*,[24] who found that for excitation densities $N < N_c = \mu^*\hbar\omega_{\mathrm{LO}}/\hbar^2$, the reduction of the exciton oscillator strength due to phase-space filling is a factor of 2 smaller than due to exciton screening. In ultrathin InAs layers N_c can be estimated as $2.4\times10^{10}\,\mathrm{cm}^{-2}$.

The nonlinearities due to the dominance of screening also become obvious in the calculations of the PT transients at different excitation densities, as shown in Fig. 2. For electron and hole concentrations of up to $3\times10^8\,\mathrm{cm}^{-2}$ rise and decay times of the transient PT and the population are virtually identical, thus reflecting the linear dependence of the bleaching on excitation density. At excitation densities larger than $10^{10}\,\mathrm{cm}^{-2}$, a plateau rather than a sharp maximum starts to emerge in the transient PT at time delays where the PT reaches its maximum. This plateau indicates that the saturation level of the inverse screening length and the exciton binding energy has been reached, where a further increase of the carrier density does not lead to a further bleaching of the absorption. At these high excitation densities, the rise time of the transient PT becomes significantly shorter than the rise time of the population, whereas the decay time of the PT transient appears to be increased. For this reason, lifetimes would be substantially overestimated, and capture times would be determined as too short if the screening contribution to the bleaching is not considered.

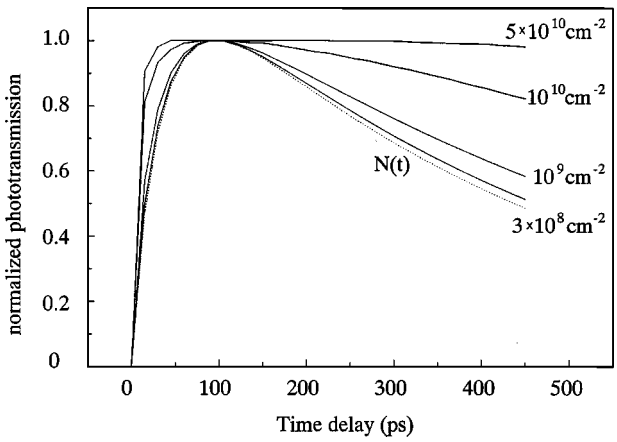

FIG. 2. Calculated phototransmission transients at the peak position of the hh exciton transition for different excitation densities (solid lines). For comparison, the transient of the population $N(t)$, which scales with the excitation density, is shown (dotted line). For excitation densities $\leqslant 3\times10^8\,\mathrm{cm}^{-2}$ the phototransmission transients directly reflect the population within 5% accuracy.

IV. RESULTS AND DISCUSSION OF THE CARRIER CAPTURE

The carrier capture measurements at the hh and lh exciton transition of the InAs layer were performed at a fixed excitation density of $2\times10^8\,\mathrm{cm}^{-2}$. The pump wavelength was set above the GaAs band gap to 1.818 eV. Figure 3 displays the PT transients in the vicinity of the lh [Fig. 3(a)] and hh [Fig. 3(b)] exciton transitions. For the measurements in the vicinity of the lh exciton transition the probe wavelength was tuned from the high-energy side of the lh transition at 1.492 eV to its low-energy side at 1.484 eV. As can be seen in Fig. 3(a), both transients exhibit the same capture time of 20 ± 2 ps, but the decay time is 200 ps shorter at 1.492 eV. In the vicinity of the hh exciton transition the opposite behavior is observed. With the probe wavelength tuned to the low-energy side of the hh exciton transition at 1.445 eV, we find a capture time of 22 ± 2 ps. In contrast, the capture time increases to 50 ± 2 ps at the high-energy side of the hh exciton transition at 1.458 eV, but both transients show the same decay time.

Figure 4 summarizes the results for the capture times when tuning the probe wavelength through the hh and lh exciton transitions. Within the lh exciton transition we find a constant capture time of 20 ps. This is surprisingly short for such a thin layer, which provides a confinement potential on the length scale of the lattice constant. In contrast, within the hh exciton transition, an abrupt increase of the capture time from 22 ps to 50 ps is observed. The line shape of the PT spectra indicates that one observes only a bleaching of the excitonic absorption but no noticeable broadening or shift of the excitonic resonances. The latter is explained by the fact that the reduction of the exciton binding energy due to screening is compensated by band-gap renormalization[25–27] resulting from a change of the single particle states under photoexcitation.

To explain the observed increase by more than a factor of 2 of the capture time within the hh exciton transition, together with the constant capture time at the lh exciton transition, we describe the population of the confined states by

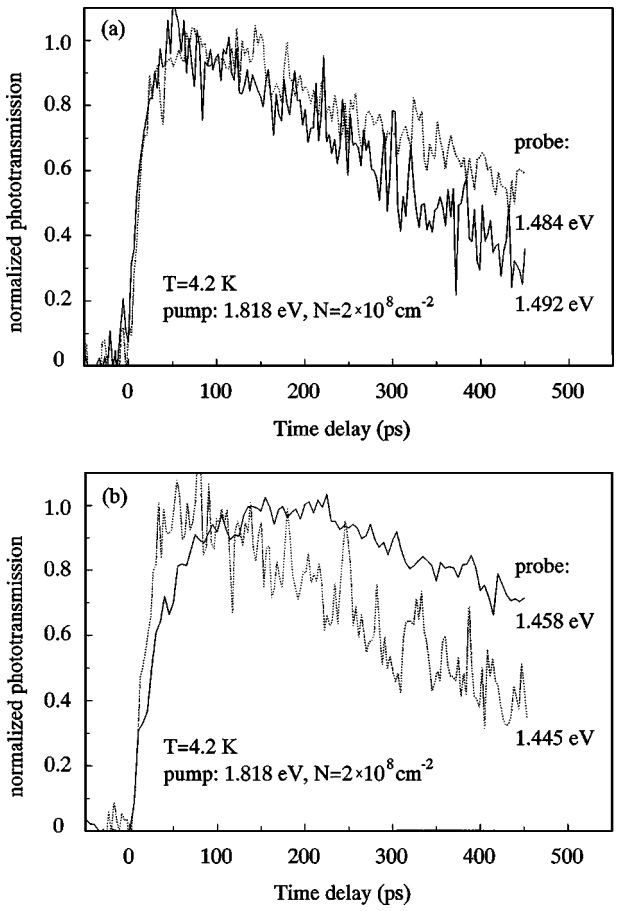

FIG. 3. Measured transient phototransmission in the vicinity of the lh exciton (top) and hh exciton transition (bottom). The probe beam was tuned from the high-energy side of the excitonic transitions (solid line) to the low-energy side (dotted line).

coupled rate equations (see Appendix A). The electron, hh, and lh states are populated by a direct capture from the GaAs barrier, expressed by the time constants for direct capture τ^{e}_{cap}, $\tau^{\mathrm{hh}}_{\mathrm{cap}}$ and $\tau^{\mathrm{lh}}_{\mathrm{cap}}$, respectively. The depopulation of these

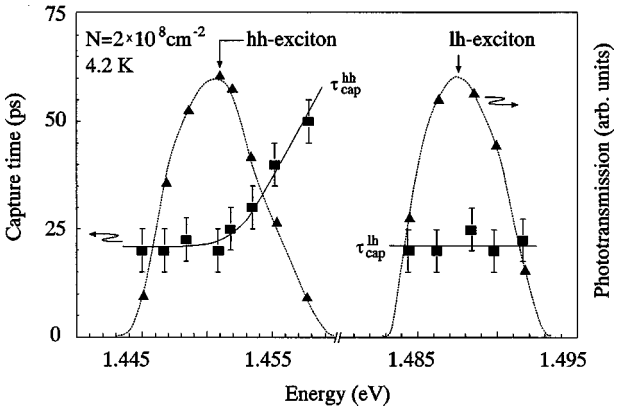

FIG. 4. Measured phototransmission rise times (■) in the vicinity of the hh and lh exciton transitions. The solid lines are a guide to the eye. Within the lh exciton transition a constant rise time of 20 ps is observed. At the hh exciton transition the rise time increases abruptly from 22 ps at the low-energy side to 50 ps at the high-energy side. The dotted lines and the symbols (▲) indicate the phototransmission spectrum.

states occurs via band-band recombination. In addition, we assume that a population of the hh level and a depopulation of the lh level can occur via intersubband relaxation from the lh state to the hh state characterized by $\tau^{\mathrm{lh-hh}}_{\mathrm{relax}}$. This approach is motivated by the results for the carrier capture[10,28] and intersubband relaxation[29] in GaAs quantum wells. The capture rates to the ground state are highest when the confining potential of the quantum well provides a bound state close to the barrier continuum and when the relaxation to the ground state can occur rapidly via LO phonon emission. In ultrathin InAs layers the situation is similar. The insertion of a 1.2-ML-thick InAs layer in a GaAs matrix leads to a confined lh state only 4.5 meV below the GaAs continuum, whereas the effective confinement energy of the hh state amounts to 42 meV.[16] Thus, the energy separation between hh and lh subbands amounts to approximately the GaAs LO phonon energy of 36 meV. As the wave functions of the confined InAs layer states extend *entirely* into the GaAs matrix, the capture process and the intersubband relaxation are well described by assuming GaAs bulk phonons. Both properties should give rise to a fast relaxation of carriers from a lh level to a hh level by LO phonon emission[29,30] within less than 1–2 ps. In contrast, when the hh-lh level separation becomes smaller than the LO phonon energy, $\tau^{\mathrm{lh-hh}}_{\mathrm{relax}}$ should increase to several tens of picoseconds.[31–33]

In order to demonstrate that a change of $\tau^{\mathrm{lh-hh}}_{\mathrm{relax}}$ from 1–2 ps to several tens of picoseconds is responsible for the observed increase of the capture time within hh exciton transition, we performed a systematic study of the parameters entering the rate equations (see Appendix B). This is necessary because rise and decay times of the populations $p_{\mathrm{hh}}(t)$ and $p_{\mathrm{lh}}(t)$ are determined by a combination of the individual hole capture times to the hh and lh level, the relaxation time for intersubband relaxation from the lh to the hh level, and the band-band recombination time. Changes in the electron capture time were not considered in this parameter study. Since the InAs layer provides only a single bound electron state, alterations of τ^{e}_{cap} would change the capture times at the hh and lh exciton transition in the same way.

Calculation of the PT transients at the hh and lh exciton transitions [see Figs. 5(a)–5(d) and Figs. 6(a)–6(d)] reveals the following conclusions.

(i) The rise time of the lh PT transient is completely insensitive to any changes of the time constant for a direct capture of holes to the confined hh level $\tau^{\mathrm{hh}}_{\mathrm{cap}}$ and the intersubband relaxation time $\tau^{\mathrm{lh-hh}}_{\mathrm{relax}}$. Therefore, the measured rise time of the PT transient at the lh exciton transition directly yields a capture time to the lh level of 20 ps.

(ii) With this value known, only an increase of the intersubband relaxation time from 2 ps to 55 ps, combined with a negligible direct capture by the hh level [see Fig. 5(b) and Fig. 6(b)], results in an increase of the PT rise time at the hh exciton transition from 22 ps to 50 ps accompanied by a decrease of lh transient decay time and a constant hh transient decay time.

At the low-energy side of the hh exciton transition, the associated hh states are populated within less than 2 ps by a fast relaxation of holes from the lh states via emission of GaAs LO phonons. This finding is agreement with experimental and theoretical studies of the intersubband relaxation

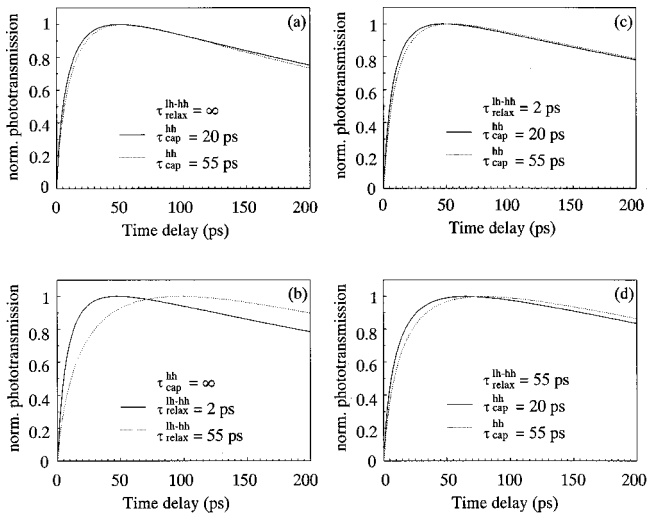

FIG. 5. Calculated transient phototransmission at the hh exciton transition according to the parameters study in Appendix B. The capture and relaxation times used in the calculations are given in the figure. The comparison of (a)–(d) reveals that only a negligible direct capture of holes to the confined hh state accompanied with a change of the relaxation time from 2 ps to 55 ps leads to an increase of the phototransmission rise time from 22 ps to 50 ps.

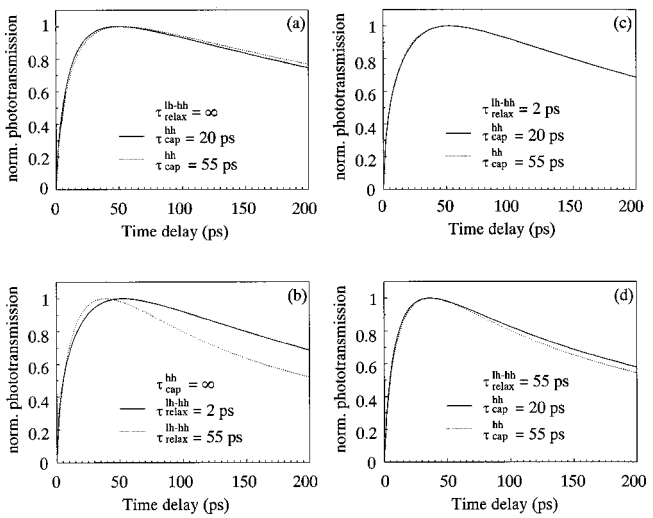

FIG. 6. Calculated transient phototransmission at the lh exciton transition using the same parameters as in Fig. 5. The comparison with Fig. 5 shows that an increase of the relaxation time from 2 ps to 55 ps leading to an increase of the hh phototransmission rise time, correlates with a reduction of the decay time of the phototransmission at the lh exciton transition.

in GaAs/AlGaAs quantum wells, which revealed relaxation times as short as 160 fs to 2 ps when the subband splitting became larger than the threshold energy for LO phonon emission.[29,30] In our case, the fast relaxation via GaAs phonons rather than InAs phonons is explained by the fact that the GaAs phonon modes are only weakly perturbated by the thin InAs layer and that the wave functions of the confined hh and lh states extend entirely into the GaAs matrix. This has previously been demonstrated in resonant luminescence experiments[34,35] on a sample similar to that used in this study.

At the high-energy side of the hh exciton transition the relaxation of holes from lh to hh levels is slowed down to more than 50 ps, but the direct capture of holes by the hh states is still not significant. The slower relaxation time is consistent with the energy separation between lh states and these hh states being smaller than the threshold energy for LO phonon emission. In such a case relaxation occurs via a cascade of acoustic phonons[31–33] with relaxation times larger than 40 ps. We therefore conclude, that a change in the relaxation mechanism from LO phonon emission to an acoustic phonon cascade, at the threshold energy of 36 meV, is sufficient to explain the observed sudden increase of the hh transient rise time accompanied by the decrease of the lh transient decay time and a constant decay time of the hh transient.

The efficient capture of holes by the confined lh state, and the relative unimportance of a direct capture by the confined hh state, can be understood as follows: assuming the capture process to take place between an initial three-dimensional and a final two-dimensional state by the emission of a LO phonon, the capture probability increases with the barrier penetration length and the density of states of the confined InAs layer states. For the 1.2-ML-thick InAs layer, the 4.5-meV effective confinement energy of the lh yields a lh barrier penetration length of 120 Å, whereas the barrier penetration length of the hh amounts to only 25 Å. In addition, the lh level possesses a larger in-plane effective mass than the hh level leading to a more than two times larger density of states for the lh. The efficient capture to the lh state results from its large barrier penetration length and its in-plane effective mass being the largest among all three confined states. In turn, the capture probability for the hh state is more than ten times smaller than that for the lh level. Since the effective hh confinement energy exceeds the LO phonon energy, transitions from a GaAs barrier state to the hh level can only occur at large final-state momentum values, which further reduces the capture probability.

V. CONCLUSIONS

In conclusion, we have shown that in the investigated ultrathin InAs layer the hole capture occurs as a two-step process where the confined lh level acts as an intermediate capture state. After the arrival of the pump pulse and relaxation of the carriers within the GaAs barrier, the holes are captured by the lh state. It is important for the subsequent cooling whether the energy separation between the lh state and an unoccupied hh state is smaller or larger than the GaAs LO phonon energy. For an energy separation larger than 36 meV, cooling to the hh level occurs within 2 ps under the emission of LO phonons. This leads to a capture time as short as 20 ps at the low-energy side of the hh exciton transition. As the energy separation decreases, however, cooling involves acoustic phonons and slows down to 50 ps. In our structure the hh and lh exciton transitions exhibit an energy separation of approximately one LO phonon. Thus, a small spectral detuning of the probe wavelength towards higher energies within the hh exciton transition leads to the observed sudden increase of the capture time.

ACKNOWLEDGMENTS

This work was part of the research program of the Dutch Foundation for Fundamental Research on Matter (FOM),

which was financially supported by the Dutch Organization for the Advancement of Research (NWO).

APPENDIX A: COUPLED RATE EQUATIONS

Assuming that, within the time resolution of the experiments, the photogenerated carriers are relaxed to within $\hbar\omega_{\mathrm{LO}}$ above the GaAs band edges, the temporal generation function can be approximated by a δ function. The temporal evolution of the electron and hole population in the GaAs barrier $n_b(t)$ and $p_b(t)$, respectively, can then be described by

$$\frac{dn_b}{dt} = n_0 \times \delta(t) - \frac{n_b}{\tau_{\mathrm{rec}}^{\mathrm{GaAs}}} - \frac{n_b}{\tau_{\mathrm{cap}}^{c}}, \tag{A1}$$

$$\frac{dp_b}{dt} = p_0 \times \delta(t) - \frac{p_b}{\tau_{\mathrm{rec}}^{\mathrm{GaAs}}} - \frac{p_b}{\tau_{\mathrm{cap}}^{\mathrm{lh}}} - \frac{p_b}{\tau_{\mathrm{cap}}^{\mathrm{hh}}}, \tag{A2}$$

where n_0, p_0 denote the number of electrons and holes initially pumped into the barrier. Using this approach, an alteration of the capture rates to the confined InAs states, due to further thermalization of carriers in the barrier, is excluded. As a depopulation mechanism for the barrier states, we consider ordinary band-band recombination ($\tau_{\mathrm{rec}}^{\mathrm{GaAs}}$) and the direct capture of electrons and holes to the confined electron, hh, and lh states of the InAs layer, expressed by the capture times τ_{cap}^{e}, $\tau_{\mathrm{cap}}^{\mathrm{lh}}$ and $\tau_{\mathrm{cap}}^{\mathrm{hh}}$, respectively. For the confined electron, hh, and lh states of the InAs layer the rate equations can be derived in a similar way as

$$\frac{dn}{dt} = \frac{n_b}{\tau_{\mathrm{cap}}^{e}} - \frac{n}{\tau_{\mathrm{rec}}^{e-\mathrm{hh}}} - \frac{n}{\tau_{\mathrm{rec}}^{e-\mathrm{lh}}}, \tag{A3}$$

$$\frac{dp_{\mathrm{hh}}}{dt} = \frac{p_b}{\tau_{\mathrm{cap}}^{\mathrm{hh}}} + \frac{p_{\mathrm{lh}}}{\tau_{\mathrm{relax}}^{\mathrm{lh-hh}}} - \frac{p_{\mathrm{hh}}}{\tau_{\mathrm{rec}}^{e-\mathrm{hh}}}, \tag{A4}$$

$$\frac{dp_{\mathrm{lh}}}{dt} = \frac{p_b}{\tau_{\mathrm{cap}}^{\mathrm{lh}}} - \frac{p_{\mathrm{lh}}}{\tau_{\mathrm{relax}}^{\mathrm{lh-hh}}} - \frac{p_{\mathrm{lh}}}{\tau_{\mathrm{rec}}^{e-\mathrm{lh}}}. \tag{A5}$$

All three subbands are populated by the direct capture of electron and holes, whereas the depopulation occurs via band-band recombination, which may differ for hh's ($\tau_{\mathrm{rec}}^{e-\mathrm{hh}}$) and lh's ($\tau_{\mathrm{rec}}^{e\text{-}\mathrm{lh}}$). In addition, the hh level can be populated by relaxation of holes from the lh states, taking place within the intersubband relaxation time $\tau_{\mathrm{relax}}^{\mathrm{lh-hh}}$.

APPENDIX B: PARAMETER STUDY

In the parameter study of $\tau_{\mathrm{cap}}^{\mathrm{hh}}$ and $\tau_{\mathrm{relax}}^{\mathrm{lh-hh}}$ one must consider the following four cases, which are related to the observed sudden increase of the capture time at the hh exciton transition.

(i) Direct hole capture by the hh and lh levels, but negligible relaxation from the lh level to the hh level. Assuming a constant electron capture time, the increase of the PT rise time within the hh exciton transition would then originate from an increase of $\tau_{\mathrm{cap}}^{\mathrm{hh}}$ from 20 ps to more than 50 ps within a 10-meV change in the hh effective confinement energy. The calculated PT transients at the hh and lh exciton transition for this case are displayed in Fig. 5(a) and Fig. 6(a), respectively. The increase of $\tau_{\mathrm{cap}}^{\mathrm{hh}}$ would be motivated by a capture time oscillating as a function of effective confinement energy, as in the case of usual quantum wells before the well provides the next confined state.[10,16]

(ii) Direct capture of holes to the confined lh level, but negligible direct capture of holes to the hh level, accompanied with a change in the hole intersubband relaxation time from 2 ps to 55 ps. The calculated PT for this case is given in Fig. 5(b) and Fig. 6(b). The drastic change in relaxation time is a consequence of the change in relaxation mechanism from GaAs LO phonon emission to an acoustic phonon cascade.

(iii) Direct capture of holes to the confined hh and lh levels, where $\tau_{\mathrm{cap}}^{\mathrm{hh}}$ increases from 20 ps to more than 50 ps towards the high-energy side of the hh exciton transition, combined with a fast carrier relaxation by LO phonon emission with $\tau_{\mathrm{relax}}^{\mathrm{lh-hh}} \leqslant 2$ ps [see Figs. 5(c) and 6(c)].

(iv) Direct capture of holes to the confined hh and lh levels, where $\tau_{\mathrm{cap}}^{\mathrm{hh}}$ increases from 20 ps to more than 50 ps at the high-energy side of the hh exciton transition, combined with a slow carrier relaxation via acoustic phonon emission with $\tau_{\mathrm{relax}}^{\mathrm{lh-hh}} \geqslant 50$ ps [see Fig. 5(d) and Fig. 6(d)]. Comparison between (iii) and (iv) also treats the case that holes are captured by the hh level as fast as by the lh level ($\tau_{\mathrm{cap}}^{\mathrm{hh}} \approx \tau_{\mathrm{cap}}^{\mathrm{lh}} = 20$ ps), and that the relaxation mechanism changes from LO phonon emission to an acoustic phonon cascade.

The PT transients were calculated with a recombination lifetime of 485 ps as found in previous time-correlated single-photon counting experiments.[35] For τ_{cap}^{e} and $\tau_{\mathrm{cap}}^{\mathrm{lh}}$ we used 20 ps, as found in the vicinity of the lh exciton transition. The comparison of Fig. 5 and Fig. 6 shows that for the hh PT transients, there are only two cases that lead to a significant increase of its rise time. In the first case, the PT rise time increases from 20 ps to 35 ps when $\tau_{\mathrm{cap}}^{\mathrm{hh}}$ increases from 20 ps to 55 ps combined with an increase of the lh to hh level relaxation time from 2 ps to 55 ps [see Figs. 5(c) and 5(d)]. This, however, leads to equal decay times in the PT transients of the lh exciton [see Figs. 6(c) and 6(d)]. In the second case, direct capture of holes to the hh level is assumed to be absent. From Fig. 6(b), it can be seen that the increase in the hh PT rise time is then accompanied by a decrease of the lh transient decay time, as observed in the experiments.

*Present address: ASM Lithography, De Run 1110, 5503 LA Veldhoven, The Netherlands.

[1] M. Alonso, M. Ilg, and K. Ploog, Phys. Rev. B **50**, 1628 (1994).
[2] M. V. Belousov, N. N. Ledentsov, M. V. Maximov, P. D. Wang, I. N. Yassievitch, N. N. Faleev, I. A. Kozin, V. M. Ustinov, P. S. Kop'ev, and C. M. Sotomayor Torres, Phys. Rev. B **51**, 14 346 (1995).
[3] P. D. Wang, N. N. Ledentsov, C. M. Sotomayor Torres, I. N. Yassievitch, A. Pakhomov, A. Yu. Egorov, P. S. Kop'ev, and V. M. Ustinov, Phys. Rev. B **50**, 1604 (1994).
[4] P. D. Wang, N. N. Ledentsov, C. M. Sotomayor Torres, P. S. Kop'ev, and V. M. Ustinov, Appl. Phys. Lett. **64**, 1526 (1994).

[5] R. Cingolani, O. Brandt, L. Tapfer, G. Scarmaccio, G. C. LaRocca, and K. Ploog, Phys. Rev. B **42**, 3209 (1990).
[6] O. Brandt, H. Lage, and K. Ploog, Phys. Rev. B **45**, 4217 (1992).
[7] N. N. Ledentsov, P. D. Wang, C. M. Sototmayor Torres, A. Yu. Egorov, M. V. Maximov, V. M. Ustinov, A. E. Zhukov, and P. S. Kop'ev, Phys. Rev. B **50**, 12 171 (1994).
[8] M. Sato and Y. Horikoshi, J. Appl. Phys. **66**, 851 (1989).
[9] M. Nakayama, T. Fujita, I. Tanaka, H. Nishimura, and H. Terauchi, Jpn. J. Appl. Phys., Part 1 **32**, 160 (1993).
[10] J. A. Brum and G. Bastard, Phys. Rev. B **33**, 1420 (1986).
[11] O. Heller and G. Bastard, Phys. Rev. B **54**, 5629 (1996).
[12] P. W. M. Blom, C. Smit, J. E. M. Haverkort, and J. H. Wolter, Phys. Rev. B **47**, 2072 (1993).
[13] T. C. Damen, M. Fritze, A. Kastalsky, J. E. Cunningham, R. N. Pathak, H. Wang, and J. Shah, Appl. Phys. Lett. **67**, 515 (1995).
[14] O. Brandt, L. Tapfer, K. Ploog, M. Hohenstein, and F. Phillipp, Phys. Rev. B **41**, 12 599 (1990).
[15] C. Giannini, L. Tapfer, S. Lagomarsino, J. C. Bouillard, A. Taccoen, B. Capelle, M. Ilg, O. Brandt, and K. Ploog, Phys. Rev. B **48**, 11 496 (1993).
[16] J. Brübach, A. Yu. Silov, J. E. M. Haverkort, W. van der Vleuten, and J. H. Wolter, Phys. Rev. B **59**, 10 315 (1999).
[17] I. Yassievitch and U. Rössler, J. Phys.: Condens. Matter **32**, 7927 (1994).
[18] S. Schmitt-Rink, D. S. Chemla, and D. A. B. Miller, Phys. Rev. B **32**, 6601 (1985).
[19] F. Stern and W. E. Howard, Phys. Rev. **163**, 816 (1967).
[20] J. Lee, H. N. Spector, and P. Melman, J. Appl. Phys. **58**, 1893 (1985).
[21] O. Hipolito and V. B. Campos, Phys. Rev. B **19**, 3083 (1979).
[22] J. A. Brum, G. Bastard, and C. Guillemot, Phys. Rev. B **30**, 905 (1984).
[23] R. Zimmermann, Phys. Status Solidi B **146**, 371 (1988).
[24] M. J. Snelling, P. Perozzo, D. C. Hutchings, I. Galbraith, and A. Miller, Phys. Rev. B **49**, 17 160 (1994).
[25] S. Hunsche, H. Hessel, A. Ewertz, H. Kurz, and J. H. Collet, Phys. Rev. B **48**, 17 818 (1993).
[26] J. Nunnenkamp, J. H. Collet, J. Klebniczki, J. Kuhl, and K. Ploog, Phys. Rev. B **43**, 14 047 (1991).
[27] L. Bányai and S. W. Koch, Z. Phys. B: Condens. Matter **63** , 283 (1986).
[28] S. V. Kozyrev and A. Ya. Shik, Fiz. Tekh. Poluprovodn. **19**, 1667 (1985) [Sov. Phys. Semicond. **19**, 1024 (1985)].
[29] S. Hunsche, K. Leo, H. Kurz, and K. Köhler, Phys. Rev. B **50**, 5791 (1994).
[30] M. C. Tatham, J. F. Ryan, and C. T. Foxon, Phys. Rev. Lett. **63**, 1637 (1989).
[31] J. A. Levenson, G. Dolique, J. L. Oudar, and I. Abram, Phys. Rev. B **41**, 3688 (1990).
[32] R. A. Höpfel, R. Rodrigues, Y. Iimura, T. Yasui, Y. Segawa, Y. Aoyagi, and S. M. Goodnick, Phys. Rev. B **47**, 10 943 (1993).
[33] A. Seilmeir, H.-J. Hübner, G. Abstreiter, G. Weimann, and W. Schlapp, Phys. Rev. Lett. **59**, 1345 (1987).
[34] P. D. Wang, N. N. Ledentsov, C. M. Sotomayor Torres, A. E. Zhukov, P. S. Kop'ev, and V. M. Ustinov, J. Appl. Phys. **79**, 7164 (1996).
[35] J. Brübach, J. E. M. Haverkort, J. H. Wolter, P. D. Wang, N. N. Ledentsov, C. M. Sotomayor Torres, A. E. Zhukov, P. S. Kop'ev, and V. M. Ustinov, J. Opt. Soc. Am. B **13**, 1224 (1996).